Surface relaxation in $c(2\times2)$Cl/Ni(100) determined by the soft-x-ray standing-wave method combined with surface-extended x-ray-absorption fine-structure spectroscopy

T. Yokoyama, Y. Takata, and T. Ohta
Department of Materials Science, Faculty of Science, Hiroshima University, Naka-ku, Hiroshima 730, Japan

M. Funabashi
Research Development Corporation of Japan, Tokodai, Tsukuba, Ibaraki 300-26, Japan

Y. Kitajima
Photon Factory, National Laboratory for High Energy Physics, Oho, Tsukuba, Ibaraki 305, Japan

H. Kuroda
Department of Chemistry, Faculty of Science, the University of Tokyo, Bunkyo-ku, Tokyo 113, Japan
(Received 5 March 1990)

The surface structure of $c(2\times2)$Cl/Ni(100) has been investigated by means of the soft-x-ray standing-wave (SW) method and surface-extended x-ray-absorption fine-structure (SEXAFS) spectroscopy. In the SW experiment, measurements of Ni(200) Bragg reflectivities in the vicinity of normal incidence allowed the determination of the mosaic width of 0.3° of the Ni(100) crystal employed, and the Cl K fluorescence yield spectrum revealed that Cl atoms are located 1.80 ± 0.03 Å above the Ni(200) lattice plane. On the other hand, the SEXAFS results elucidated that the Cl-Ni layer spacing is 1.60 ± 0.02 Å. Combining these data, it was found that the surface nickel layer relaxes outward by 0.20 ± 0.05 Å (11% of the bulk spacing).

I. INTRODUCTION

The x-ray standing-wave (SW) method is a powerful technique for determining surface structure, and a number of works using hard x rays have been published.[1-6] For example, Berman *et al.*[5] recently investigated the surface structure of submonolayer Au/Si(111) from the x-ray SW triangulation method, which can predict three-dimensional structures, and concluded that Au atoms are located at an unusual adsorption site, which is embedded in the substrate and bridges two Si atoms in the lower half of the (111) double layer.

On the contrary, the soft-x-ray SW method is less common because the light source of soft x rays has been very limited. Recently, however, several facilities supplying tunable and intense soft x rays have been developed by use of synchrotron radiation, and the utility of the soft-x-ray SW method has been pointed out. Ohta *et al.*,[7,8] Woodruff *et al.*,[9] and Yokoyama *et al.*[10,11] have remarked that the soft-x-ray SW method has several advantages in comparison with the hard-x-ray method. The full width at half maximum (FWHM) of a Bragg reflection becomes significantly larger as the Bragg angle approaches 90°, and by use of soft x rays we can make an incident x ray normal to the lattice plane for most metal and semiconductor crystals. This fact enables us to apply this method to mosaic crystals whose SW data are difficult to obtain by use of hard x rays. Furthermore, the soft-x-ray SW method does not require highly collimated x rays, and therefore we can utilize soft-x-ray beamlines for experiments such as extended x-ray-absorption fine structure (EXAFS) without any modification, and also use standard ultrahigh vacuum (UHV) chambers for the studies of solid surfaces.

Woodruff *et al.*[9] presented the first application of this method to Cl/Cu(111) and successfully demonstrated that Cl atoms are adsorbed at the threefold-hollow site and the spacing between adsorbate Cl and bulk Cu layers is 1.81 Å, which is consistent with their surface-EXAFS (SEXAFS) and photoelectron diffraction data. The present authors[10] remarked that the magnitude of surface relaxation can be quantitatively estimated by combining the SW and SEXAFS techniques by analyzing the data of $p(2\times2)$S/Ni(111). Very recently, Patel *et al.*[12] investigated the surface relaxation appearing in $c(2\times2)$Cl and $p(2\times2)$S/Cu(100) by the combined method, and found a 0.07 ± 0.04 Å outward relaxation in the Cl-covered surface.

Nakahata *et al.*,[13] Patel *et al.*,[12] and Yokoyama *et al.*[11] previously reported Bragg reflectivities in the normal-incident geometry. It is quite useful to measure Bragg reflectivities in order to determine the mosaic spread of a crystal employed as well as to verify the energy resolution of incident x rays. Patel *et al.*[12] and Yokoyama *et al.*[10,11] further mentioned that it is of great importance to record the yield spectrum from adsorbates with sufficiently high signal-to-background (SB) ratio. For instance, the Auger electron yield mode may not be a good candidate since the background electrons which originate from substrates provide strong SW signals and disturb the adsorbate ones. For reliable measurements of the SW profiles from adsorbates, fluorescence yield detection, which usually gives high SB ratio, is often superior to the Auger yield method.

In this paper, the detailed results of the soft-x-ray SW and SEXAFS experiments for $c(2\times2)$Cl/Ni(100) are described. In Sec. II, experimental details of the sample preparation and spectroscopic measurements are given. Sections III and IV deal with the results of the SW and SEXAFS analysis, respectively, and in Sec. V we discuss the detailed surface structure accompanied by surface relaxation.

II. EXPERIMENTAL DETAILS

A Ni(100) single crystal (10-mm diameter) was mechanically and electrochemically polished, and then mounted in an UHV chamber, whose base pressure was less than 1×10^{-10} mbar during the experiments. The crystal was cleaned by the repeated cycles of Ar^+ bombardment and annealing at about 1000 K, and the surface cleanliness and order were verified with Auger electron spectroscopy (AES) and low-energy electron diffraction (LEED), respectively. The clean crystal was subsequently dosed with Cl_2, which was prepared by the electrolysis of sintered AgCl.[14] The pressure was less than 2×10^{-10} mbar throughout dosing of Cl_2. Complete saturation of chlorine adsorption yielded $c(2\times2)$ structure, and the LEED pattern retained its sharpness even after all the measurements.

Spectroscopic measurements were performed at the soft-x-ray double-crystal monochromator station Beamline 11B (Ref. 15) of the Photon Factory in the National Laboratory for High Energy Physics (KEK-PF). Synchrotron radiation emitted from a normal bending magnet is first reflected by a bent cylindrical mirror and is monochromatized by a pair of InSb(111) crystals. The x rays obtained are collimated by several apertures, and its divergence is estimated to be less than 1 mrad and the beam size at the sample crystal was about 2×4 mm^2. The first crystal was water cooled to avoid the change of the lattice spacing and also radiation damages.[16] By the rocking-curve measurement, the energy resolution of the InSb(111) crystals was determined to be 2.0 eV at 3500 eV [in the vicinity where the normal incidence Ni(200) Bragg reflection occurs].

Ni(200) Bragg reflectivities were recorded by monitoring photoelectric current I_G from the Cu grid in front of the clean crystal. Experimental setup is depicted in Fig. 1. The photoelectric current I_G can be expressed as an equation such that

$$I_G = I_0(1+TR)\ , \tag{1}$$

where I_0 is the intensity of an incident beam, R is the Bragg reflectivity, and T is the transmission ratio of a Cu grid (0.8 in the present case). Reflectivity curves were recorded at several angles close to normal incidence in order to estimate the mosaicity of the crystal. At the ring operation of 2.5 GeV and 350–180 mA, the photoelectric current I_G was in the range of 0.3×10^{-10} A without supplying voltage to the Cu grid. This allowed fast measurements of reflectivities (about 5 sec/point) with good signal-to-noise (SN) ratio.

A Cl K fluorescence yield spectrum was recorded at the incident angle of 85.0° by use of an UHV-compatible gas-flow proportional counter (FPC),[17] which is shown in Fig. 1. The detector was placed to collect soft x-rays of glancing emission from the sample crystal, and the count rate of Cl K fluorescence was around 1000 counts/sec. Figure 2 shows pulse-height spectra from the present FPC. When the photon energy of primary x ray is 2800 eV (below the Cl K edge), there appear small amounts of signals attributed to elastic scattering. Just above Cl K edge (2854 eV), the Cl K fluorescence signal dominates the spectrum, and as the incident photon energy increases, Cl K fluorescence gradually decreases while the elastic scattering signal becomes intense. Although the energy of Cl K fluorescence (2621 eV) was fairly apart from that of Ni L (851 eV), the elastic scattering peak ap-

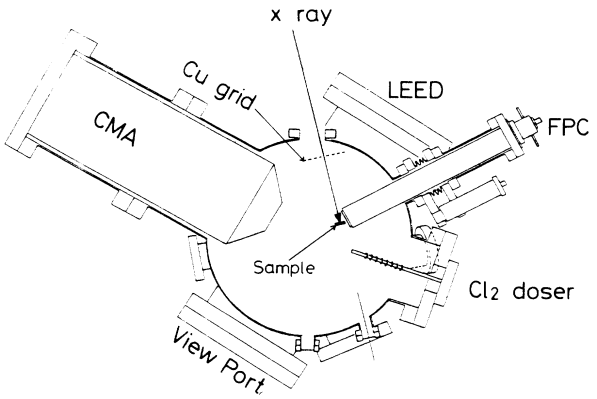

FIG. 1. Experimental setup for the soft-x-ray standing-wave measurements. The Cu grid in front of the sample crystal measures the total intensity of the incident and reflected x rays. A fluorescence yield from an adsorbate is measured by the gas-flow proportional counter, and a total electron yield spectrum is taken by the direct photocurrent from the sample crystal.

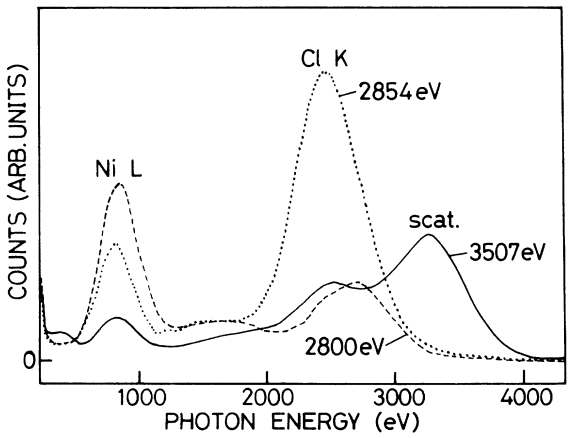

FIG. 2. Energy distribution curves of soft x rays emitted from a $c(2\times2)$Cl-covered Ni(100) single crystals by irradiating monochromatized beam. Photon energies of the primary soft x rays are 2800 eV (below Cl K edge), 2854 eV (just above Cl K edge), and 3507 eV (the SW region). Small onset appearing at about 1600 eV is ascribed to Si K fluorescence, which may originate from insulating materials and viewing ports in the sample chamber.

pearing strongly at the spectrum of 3507 eV cannot be distinguished completely from Cl K fluorescence. The raw fluorescence yield spectrum which has been obtained by filtering with an appropriate SCA (single channel analyzer) window therefore contains the component of elastic scattering. In order to subtract the contribution of elastic scattering signals, a pulse-height spectrum and a yield spectrum from a clean Ni(100) crystal were also recorded on the same condition. By comparing the pulse-height spectra, the resultant SB ratio was found to be 250%. Note that the SB ratio in Auger electron yield spectra is only about 10%. The background contribution appearing in the yield spectrum of the clean Ni(100) was subsequently subtracted from the raw fluorescence yield spectrum to give a normalized SW spectrum. In order to calibrate the incident angle and photon energy of a monochromatized beam, a reflectivity spectrum was recorded simultaneously. A total electron yield spectrum was also taken for the substrate spectrum by monitoring photocurrent (in the range of 1×10^{-10} A) from the sample crystal.

Polarization-dependent Cl K edge SEXAFS spectra were measured at room temperature by varying the direction of the incident **E** vector. The same proportional counter was used to obtain fluorescence yield spectra. Cl K fluorescence intensities were normalized with the intensity of incident x rays, I_0, which was measured with the photocurrent from the sample crystal. To obtain the backscattering amplitude and phase shift of a Cl-Ni pair, a Cl K edge EXAFS spectrum of CuCl was taken at 140 K instead of $NiCl_2$, since $NiCl_2$ may be too hygroscopic to measure the spectrum with a total electron yield mode. Here it is assumed that the backscattering amplitude of Cu is essentially the same as that of Ni. A low-temperature measurement is required for CuCl because of its large anharmonic vibrations around room temperature.

III. RESULTS OF SW ANALYSIS

Figure 3 shows the incident angle dependence of observed Bragg reflectivities, together with calculated ones. It clearly shows that the maximum reflectivity gradually decreases and the FWHM increases with the decrease in the incident angle, due to the finite mosaic spread of the present crystal. One can determine the energy resolution of incident x rays and the mosaic width of the present Ni(100) crystal by analyzing the reflectivity spectra. The basic theory and formulation of x-ray standing waves have been presented in the literature,[18–20] and Woodruff *et al.*[7] and Hashizume *et al.*[21] showed that particular forms of the expressions relevant to the experimental conditions of the energy-scanning mode and nearly normal incidence of soft x rays. Because of the finite energy resolution and mosaic spread, an observed Bragg reflectivity is expressed by convoluting a theoretical spectrum with appropriate distribution functions. One can evaluate reflectivity curves with the assumption that both the energy distribution of the incident x rays and angle distribution of the sample crystal are described with

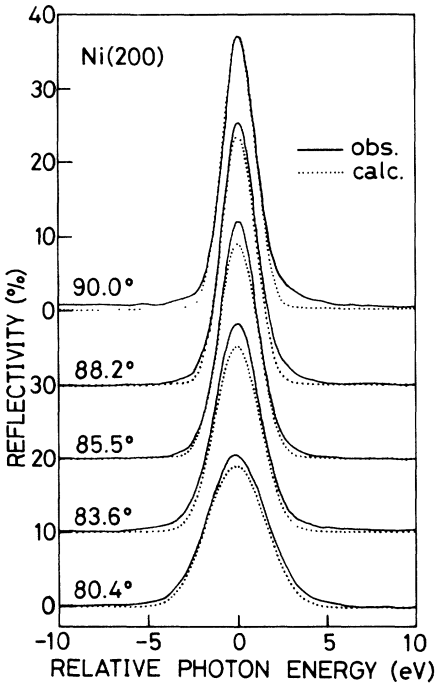

FIG. 3. The Ni(200) Bragg reflectivities from a clean Ni(100) crystal at several incident angles. The solid lines correspond to the observed data and the dotted lines to the calculated ones.

Gaussian functions.[21] Theoretical curves given in Fig. 3 were obtained when it was assumed that the energy resolution is 2.0 eV and the mosaic spread is 0.3°. Structure factors used in these calculations are $F_{000}=112.0+2.2i$ and $F_{111}=73.284+2.091i$ (including Debye-Waller factor). The calculated curves agree fairly well with the observed ones so that it can be concluded that the mosaic spread has been determined successfully. The slight deviations between the observed and calculated reflectivities may be caused mainly by the ambiguity of the incident angles, the experimental error of which is estimated to be as much as $\pm0.5°$. This does not lead to the noticeable ambiguity of the mosaic spread determined. Note that the energy resolution thus determined is in good agreement with the value obtained by the rocking-curve measurements of the monochromator crystals.

The next step is to analyze the fluorescence and total electron yield SW spectra. Figure 4 shows the observed yield spectra, together with the calculated ones. The Cl K fluorescence yield spectrum closely resembles that of the total electron yield spectrum, which is regarded as the substrate profile. This indicates that adsorbate Cl is located in the vicinity of the Ni(200) (virtual) lattice plane. Theoretical curves can be evaluated in a straightfoward way since the energy resolution and mosaic width have been determined as described above and the remaining fitting parameters to be adjusted are only the displacement relative to the lattice plane Δz and the coherent factor F_{co}. Similar Gaussian convolutions are adopted in this calculation. Figure 4 also gives the calculated spectra. For the profile of substrate Ni, both Δz(Ni) and F_{co}(Ni) were fixed to be 0.0 Å and 1.0, respectively. Although no fitting parameters are employed, the calcu-

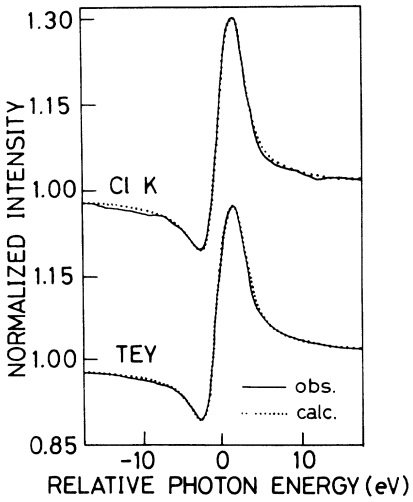

FIG. 4. Cl K fluorescence and total electron yield spectra of $c(2\times2)$Cl/Ni(100), which corresponds to the standing-wave field intensities at the vertical positions of adsorbate Cl and bulk Ni, respectively. The solid lines are the observed ones and the dotted lines are the calculated ones. In the calculated total electron yield spectrum, no adjustable parameters are employed; i.e., $\Delta z = 0.00$ Å and $F_{co}(\mathrm{Ni}) = 1.00$ are assumed. In the fluorescence yield spectrum, the refinement yields $\Delta z(\mathrm{Cl}) = 0.04$ Å and $F_{co}(\mathrm{Cl}) = 1.00$.

lated spectrum reproduces the observed one fairly well, indicating that the mosaic spread is determined with high reliability. The best fit of a profile from an adsorbate Cl yields $\Delta z(\mathrm{Cl}) = 0.04 \pm 0.03$ Å or 1.80 ± 0.03 Å and $F_{co}(\mathrm{Cl}) = 1.0$. The values of $F_{co}(\mathrm{Ni})$ and $F_{co}(\mathrm{Cl})$ indicate that not only the bulk but also the surface has well-ordered structures.

IV. RESULTS OF SEXAFS ANALYSIS

Figure 5 shows Cl K edge SEXAFS spectra of $c(2\times2)$Cl/Ni(100) at three incident angles of 90°, 45°, and 15°. These data were analyzed according to well-established procedures;[22] the EXAFS oscillation functions $k^2\chi(k)$ we first extracted by background subtraction and normalization, and were subsequently Fourier transformed into r space. In the Fourier transforms depicted in Fig. 6, the first-nearest-neighbor Cl-Ni coordination appears dominantly, and other higher coordinations are also observed. The present analysis deals only with the first-nearest-neighbor Cl-Ni. The dominant peak in each Fourier transform was filtered by multiplying a Hanning window function,[22] and was then inverse Fourier transformed into k space again. In order to derive the backscattering amplitude and phase shift of a Cl-Ni pair, the Cl K edge EXAFS spectrum of CuCl at 140 K was also analyzed in a similar manner.

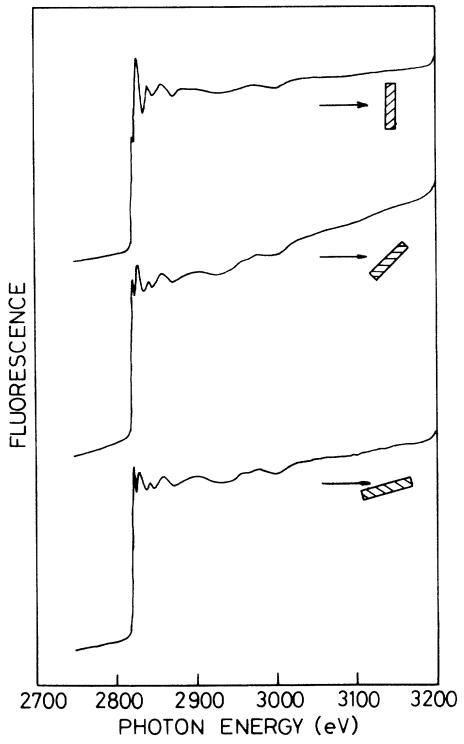

FIG. 5. Cl K-edge SEXAFS spectra of $c(2\times2)$Cl/Ni(100) taken at room temperature by means of the Cl K fluorescence yield mode. The incident angle of x rays varies from 90° to 45° and 15° with respect to the surface plane. Strong oscillations can be attributed to the first-nearest-neighbor Cl-Ni coordination.

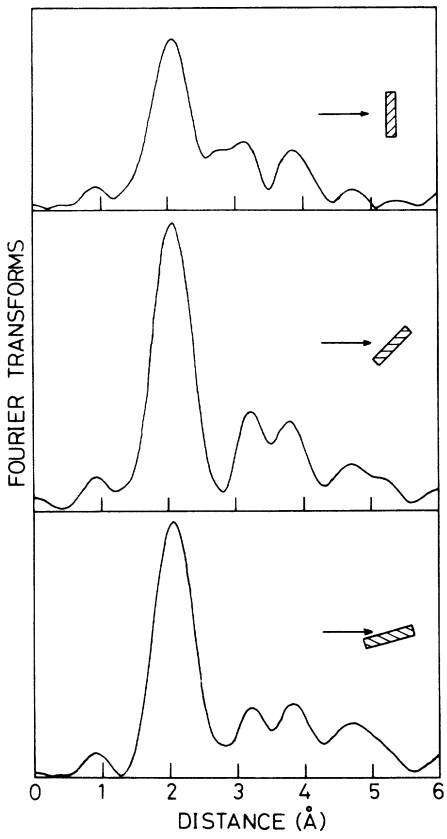

FIG. 6. Fourier transforms of EXAFS oscillation functions $k^2\chi(k)$. Although higher coordination shells are observed in each transform, only the first nearest shells are analyzed.

TABLE I. SEXAFS results of the interatomic distance R and the effective coordination number N^* for the first-nearest-neighbor Cl-Ni coordination. The calculated effective coordination number for each adsorption site is given in order to verify the Cl location, with the assumption of the Cl-Ni distance of 2.38 Å. The ratio of N^* is also tabulated in the last two rows.

	Experimental		Calculated N^*		
Angle (deg)	R (Å)	N^*	hollow	bridge	atop
90	2.39	3.04	3.29	0.82	0.00
45	2.38	4.98	4.36	2.59	1.50
15	2.37	4.63	5.28	4.12	2.80
90/15		0.66	0.62	0.20	0.00
45/15		1.08	0.83	0.63	0.54

The extracted $k^2\chi(k)$ was curve fitted to yield structure parameters such as effective coordination numbers and interatomic distances. A mean-square relative displacement $\Delta\sigma^2$ was assumed to be larger by 3.00×10^{-3} Å^2 than that of the reference. This assumption yielded the satisfactory fits for all the SEXAFS spectra. The results are summarized in Table I, together with the calculated angle dependence of the effective coordination numbers for atop, bridge, and four-fold-hollow sites. The ratio of the effective coordination numbers clearly exemplifies the Cl atoms are adsorbed at the four-fold-hollow site with the Cl—Ni bond distance of 2.38 Å. Sette *et al.*[23] and Citrin[24] already reported SEXAFS results of the present system, and remarked that the adsorption site is the four-fold-hollow and the bond distance is 2.37 Å, these results being sufficiently consistent with our present data. They further determined the magnitude of surface relaxation by analyzing the higher coordination shells, and this will be discussed below.

V. DISCUSSION

The surface structure is described by the SW results combined with the SEXAFS ones. The SEXAFS results reveal that the layer spacing between Cl and Ni is 1.60±0.02 Å. This value is significantly different from the Δz value of 1.80 Å obtained by the SW analysis. This deviation indicates that there exists outward relaxation of the first Ni layer. If we assume that only the first Ni layer relaxes and other layers are fixed with the layer spacing of 1.76 Å, the surface layer spacing can be estimated to be 1.96±0.05 Å, which corresponds to the expansion of 0.20±0.05 Å compared with the bulk value. The surface structure of the present system is consequently described as in Fig. 7.

Sette *et al.*[23] have already reported the 0.12 Å expansion of the first-to-second Ni layer spacing in the same system by analyzing higher coordination shells in the SEXAFS spectra. The SW analysis includes considerably large errors judging from its lower resolving power compared with that of SEXAFS. The SEXAFS analysis, however, is also a difficult task for the higher coordination shells since multiple-scattering and/or asymmetric effects often prevent one from obtaining reliable results. Accordingly, the present deviation could be ascribed to experimental and analytical errors. Another possibility might be expansion of the second-to-third Ni layer. Since the SW data give the relative displacement of the atom of interest with respect to the bulk lattice plane, the resultant difference between the surface layer spacing and the bulk one should be regarded as the sum of layer expansions near the surface. If the second-to-third Ni layer expands to some extent, the present deviation between that of Sette *et al.* and ours should be reduced. They explained their results using simple physical concepts. The formation of an ionic Cl—Ni bond involving charge transfer from Ni to Cl should create a dipole layer with positively charged surface Ni atoms, resulting in the Coulomb repulsion between the first and second Ni layers. An alternative explanation is that the valence-band electrons that participated in the metallic bond between the first- and second-layer Ni atoms should be used to form Cl—Ni bondings, and this leads to the weakening of the Ni—Ni bonds.

In conclusion, the usefulness of the soft-x-ray SW method is emphasized. The same optical system and the same UHV chamber with a fluorescence detector as those for surface EXAFS experiments can be used. Although the present experimental error could be further reduced by use of a much more highly resolving monochromator, the soft-x-ray SW method in this work gave useful information on surface structure. These two techniques provide complementary information; surface-EXAFS spectroscopy gives local structures such as interatomic distances between adsorbates and substrate surfaces, while the SW method provides the displacement of adsorbates relative to the net plane of the bulk substrate. Combining these methods, we can elucidate the whole surface structure of adsorbate-substrate systems.

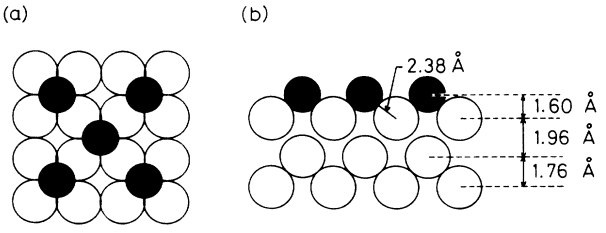

FIG. 7. Schematic representation of the top (a) and the side (b) views of $c(2\times2)$Cl/Ni(100). Solid circles denote chlorine atoms while open circles exhibit nickel atoms. Note that the spacing of the first-to-second nickel layer expands by 0.20±0.05 Å.

ACKNOWLEDGMENTS

The authors acknowledge Dr. P. H. Citrin of AT&T Bell Laboratory for his detailed and valuable suggestions on our SEXAFS analysis. They also thank Dr. S. Hino for Chiba University for his kind advice about the Cl_2 doser. One of us (T.O.) is grateful for the financial support of the Grant-in-Aid for Scientific Research (No. 63609002). This work has been performed under the approval of the Photon Factory Program Advisory Committee (Proposals No. 87-139 and No. 88-189).

[1]P. L. Cowan, J. A. Golovchenko, and M. F. Robbins, Phys. Rev. Lett. **44**, 1680 (1980).

[2]J. A. Golovchenko, J. R. Patel, D. R. Kaplan, P. L. Cowan, and M. J. Bedzyk, Phys. Rev. Lett. **49**, 560 (1982).

[3]P. Funke and G. Materlik, Solid State Commun. **54**, 921 (1985).

[4]G. Materlik, J. Zegenhagen, and W. Uelhoff, Phys. Rev. B **32**, 5502 (1985).

[5]L. Berman, B. Batterman, and J. Blakely, Phys. Rev. B **38**, 5397 (1988).

[6]Y. Saitoh, H. Hashizume, and K. Tsutsui, Jpn. J. Appl. Phys. **27**, 1386 (1988).

[7]T. Ohta, H. Sekiyama, Y. Kitajima, H. Kuroda, T. Takahashi, and S. Kikuta, Jpn. J. Appl. Phys. **24**, 1475 (1985).

[8]T. Ohta, Y. Kitajima, H. Kuroda, T. Takahashi, and S. Kikuta, Nucl. Instrum. Methods A **246**, 760 (1986).

[9]D. P. Woodruff, D. L. Seymour, C. F. McConville, C. E Riley, M. D. Crapper, and N. P. Prince, Phys. Rev. Lett. **58**, 1460 (1987); Surf. Sci. **195**, 237 (1988).

[10]T. Yokoyama, M. Funabashi, Y. Kitajima, T. Ohta, and H. Kuroda, Physica B **158**, 643 (1989).

[11]T. Yokoyama, Y. Takata, M. Yoshiki, T. Ohta, M. Funabashi, Y. Kitajima, and H. Kuroda, Jpn. J. Appl. Phys. **28**, L1637 (1989).

[12]J. R. Patel, D. W. Berreman, F. Sette, P. H. Citrin, J. E. Rowe, P. L. Cowan, T. Jach, and B. Karlin, Phys. Rev. B **40**, 1330 (1989).

[13]T. Nakahata, H. Hashizume, M. Oshima, and T. Kawamura, Jpn. J. Appl. Phys. **28**, L1300 (1989).

[14]N. D. Spencer, P. J. Goddard, P. W. Davies, M. Kiston, and R. M. Lambert, J. Vac. Sci. Technol. A **1**, 1554 (1983).

[15]T. Ohta, P. M. Stefan, M. Nomura, and H. Sekiyama, Nucl. Instrum. Methods A **246**, 373 (1986).

[16]M. Funabashi, M. Nomura, Y. Kitajima, T. Yokoyama, T. Ohta, and H. Kuroda, Rev. Sci. Instrum. **60**, 1983 (1989).

[17]M. Funabashi, T. Ohta, T. Yokoyama, Y. Kitajima, and H. Kuroda, Rev. Sci. Instrum. **60**, 2505 (1989).

[18]B. M. Batterman and H. Cole, Rev. Mod. Phys. **36**, 681 (1964).

[19]D. W. Berreman, Phys. Rev. B **14**, 4313 (1976).

[20]D. W. Berreman and A. T. Macrander, Phys. Rev. B **37**, 6030 (1988).

[21]H. Hashizume and T. Nakahata, Jpn. J. Appl. Phys. **27**, L1568 (1988).

[22]See, for example, *X-Ray Absorption: Principles, Applications and Techniques of EXAFS, SEXAFS, and XANES,* edited by D. C. Koningsberger and R. Prins (Wiley, New York, 1988).

[23]F. Sette, T. Hashizume, F. Comin, A. A. MacDowell, and P. H. Citrin, Phys. Rev. Lett. **61**, 1384 (1988).

[24]P. H. Citrin, private communication.